# Electric Propulsion Plasma Simulations and Influence on Spacecraft Charging

M. Tajmar*

Space Propulsion
Austrian Research Centers Seibersdorf, A-2444 Seibersdorf, Austria
Tel: +43-50550-3142, Fax: +43-50550-3366, Email: martin.tajmar@arcs.ac.at

Electric propulsion thrusters gain increasing importance for both commercial applications as well as for scientific and interplanetary spacecraft due to their high specific impulse, thrust controllability and proven reliability. However, since such type of thrusters emit charged propellant, contamination due to collision processes inside the beam and influence on spacecraft charging is a serious issue. Specifically, low-energy charge-exchange ions which can be attracted by potentials on the spacecraft surface need to be well studied. Several three-dimensional Particle-In-Cell (PIC) numerical models were developed to study Hall, Ion and FEEP thrusters covering both high and low thrust electric propulsion systems. This paper addresses the various numerical approaches (full particle model, hybrid), different potential solution implementations (Poisson solver, quasi neutral plasma assumption) related to the development of such plasma simulations. A model is derived to predict changes in spacecraft charging due to the presence of the charge-exchange plasma. Plasma environments, charge-exchange backflow currents and spacecraft charging in vacuum, LEO and GEO conditions are evaluated and discussed. Simulations suggests, that since backflow currents are very low for FEEP thrusters, a neutraliser is not always necessary to maintain the spacecraft floating potential in LEO orbits.

## 1. Introduction

Electric propulsion thrusters are now being used for many different spacecraft applications such as interplanetary, telecommunication or scientific satellites[1]. According to mission requirements, high-, medium-, and low-thrust engines are being developed. For example, a Hall thruster will fly as the primary propulsion system on the European moon satellite[2] SMART-1 (up to 88 mN), the ARTEMIS[3] telecommunication satellite is equipped with Ion thrusters (20 mN), and MICROSCOPE[4] will use a FEEP thruster (100 µN) for precise attitude control.

In addition to neutral propellant, electric propulsion thrusters emit a plasma which can interact with the spacecraft or the ambient plasma. The main interaction is caused by low velocity charge-exchange ions, produced inside the plume from collisions between fast beam ions and propellant neutrals. These ions can flow back to the spacecraft surface causing sputtering and inducing an additional current or distribute around the spacecraft which can influence plasma instrument observations. Due to chamber wall and rest gas density limitations, computer particle simulations, verified by ground and in-flight measurements, provide the best means to address this problem.

Three-dimensional Particle-In-Cell (PIC) models were developed to simulate the plasma environment of Hall, Ion and FEEP thrusters[5-9]. Monte-Carlo collisions are used to predict charge-exchange ions and to estimate the amount of current flowing back to the spacecraft. As a novel feature, virtual plasma sensors with real physical dimensions are implemented to perform accurate code verification comparisons with available data.

The models for all three types of thrusters will be summarised and examples of induced plasma environments are shown. The reader is referred to the references written above for any details about the model and simulation parameters used. A simple floating potential model is utilised to investigate the influence of the charge-exchange plasma on spacecraft charging.

## 2. Physical Models

### *2.1 Hall and Ion Thrusters*

A Hall thruster emits an ion beam out of a ring-shaped anode with a halfcone divergence of about 40°. Ion thrusters accelerate the propellant through a grid having a lower half cone divergence angle around 10°-15°. Typical operating parameters are summarised in Table 1. A schematic sketch is shown in Figure 1. Electrons from an external cathode act as a neutraliser creating a quasi-neutral plasma. Although the propellant efficiency for these type of thrusters exceed 95%, the neutral density is comparable to the beam ion density due to the much lower thermal velocities (400 m/s) compared to the ion velocities gained due to the acceleration potential of 300 V - 1100 V (20,800 – 40,000 m/s) between anode and cathode. Moreover, part of the propellant is directed through the cathode thus

* Research Scientist

| Parameters | SPT-100 | UK-10 | RIT-10 |
|---|---|---|---|
| Thrust | 84 mN | 25 mN | 15 mN |
| Voltage | 300 V | 1100 V | 1000 V |
| Mass Flow Rate | 5.6 mg/s | 0.8 mg/s | 0.4 mg/s |
| Total Efficiency | 51% | 77% | 71% |
| Divergence Angle | 42° | 12° | 11° |
| Outer Diameter | 100 mm | 100 mm | 100 mm |
| Inner Diameter | 56 mm | - | - |

**Table 1 Hall and Ion Thruster Performance Parameters**

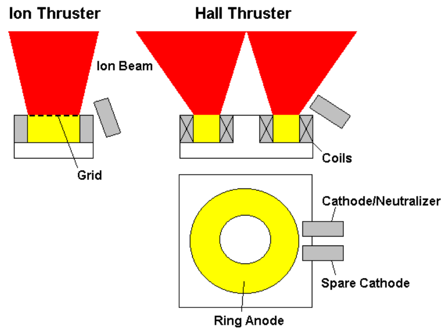


**Figure 1 Hall and Ion Thruster Schematic Sketch**

providing an additional flow of neutral propellant. Up to 20% of the ions are found to be doubly charged.

A consistent formalism between thrust, ion velocities and mass flow rates could be established which defines the conditions at the exit plane of the thrusters[7]. Ion distributions are either homogenous (Hall Thruster) or Gaussian (Ion Thruster) matching ground testing data.

Since these types of thrusters emit a quasi-neutral plasma, the electrons can be modeled as a fluid speeding up simulation time. Assuming a collisionless plasma, a constant electron temperature $T_e$ and a Boltzmann distribution of the electrons, the space charge potential $\phi$ can be calculated quickly using only ion densities

$$n_i \approx n_e = n_{e\infty} \cdot \exp\left(\frac{e\phi}{kT_e}\right) \qquad (1)$$

where $n_{e\infty}$ is the electron density in infinity calculated using exit potential measurements.

*2.2 FEEP Thrusters*

Two types of FEEP thrusters are currently under development: one using a slit shaped emitter and cesium as propellant[10] and a needle type emitter using Indium as propellant[11]. A schematic sketch of both thrusters is shown in Figure 2, performance data is summarized in Table 2.

A potential difference in the order of 6 – 12 kV is applied between emitter and accelerator electrode creating a focused ion beam squeezed inside a cosine distribution. An important difference between the two designs is, that in the slit configuration, the accelerator electrode is negative (a few kV) with respect to ground whereas in the needle design the accelerator is on ground potential. Typical divergence angles are between 20° and 60° depending on the thrust level.

Cesium, like all alkali metals, has a very high vapour pressure of $2x10^{-4}$ Pa at the melting point of 28.6° C. Moreover a high atomic neutral flux of about 1% of the ion flux was observed[12] suggesting dissociations of microdroplets that are emitted related to the efficiency of the thruster. This flux together with thermal epavoration (approximately two order below the flux) creates a considerable atomic neutral environment in front of a Cs-FEEP thruster which can cause charge-exchange ions[9].

Indium has a very low vapour pressure of only $5x10^{-11}$ Pa at the melting point of 156.8 °C. Contribution from thermal evaporation to atomic neutrals is therefore neglectible. Only sputtering from the fast beam ions on the microdroplets is considered as an additional source of atomic neutrals. A volumetric production rate based on cross section, sputter yields, ion and microdroplet measurements was implemented for this case[5].

A seperate neutraliser is needed to provide the electrons in order to keep the spacecraft potential constant[13]. Contrary to Hall and Ion thrusters, the electrons are not needed to maintain ion emission.

*2.3 Floating Potential Model*

Submerged in an ambient plasma environment, the spacecraft will charge up to a floating potential such that the electron and ion currents will balance. Due to the operation of an electric propulsion thruster, the plasma environment will be modified significantly and thus the floating potential will change. In reality, many complex phenomena contribute to spacecraft charging such as secondary electron emission or photo electron emission. Also ambient plasmas are not constant but are e.g. influenced by solar activity.

By assuming typical ambient plasma conditions (only one ambient species for simplification) we can estimate spacecraft floating potentials to a reasonable extent and investigate the influence due to the operation of electric propulsion thrusters.

The total ion current from the environment to the spacecraft consists of the thermal flux and a ram component depending on the spacecraft velocity $v_{SC}$. In

| Parameters | Cs-FEEP | In-FEEP |
|---|---|---|
| Thrust | 580 µN | 28 µN |
| Emitter Voltage | 6.5 kV | 7 kV |
| Accelerator Voltage | - 5 kV | 0 V |
| Current | 5 mA | 0.25 mA |
| Divergence Angle | 66° Perpendicular to Slit<br>20° Parallel to Slit | 50° |

**Table 2 µN FEEP Thruster Performance Parameters**

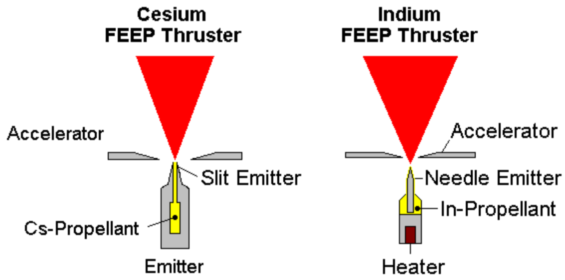


**Figure 2 FEEP Thruster Schematic Sketch**

addition, the thruster will emit a current $I_E$ and charge-exchange ions that flow back to the surface will contribute with the backflow current $I_B$. We can summarise the total ion current to the spacecraft as

$$I_i = \frac{en_\infty}{4} \cdot \sqrt{\frac{8k_B T_{e\infty}}{\pi m_i}} \cdot A_{SC} + en_\infty v_{SC} A_{ram} + I_B - I_E \qquad (2)$$

where $n_\infty$ is the ambient plasma density, $T_{e\infty}$ the ambient electron temperature and $m_i$ the ambient ion mass. We can do the same for the total electron current which also consists of a thermal flux (we assume an ambient potential of zero Volt), the current emitted by the neutraliser $I_N$ and electrons that are flowing from the charge-exchange plasma towards the spacecraft surface:

$$I_e = -\frac{en_\infty}{4} \cdot \sqrt{\frac{8k_B T_{e\infty}}{\pi m_e}} \cdot A_{SC} \cdot \exp\left(\frac{eV_f}{k_B T_{e\infty}}\right) + \iint_{SC} \frac{en_{CEX}}{4} \cdot \sqrt{\frac{8k_B T_{CEX}}{\pi m_e}} \cdot \exp\left[\frac{e(V_f - V_{CEX})}{k_B T_{CEX}}\right] dA + I_N \qquad (3)$$

where the exponential factor comes again from a Boltzmann energy distribution assumption, $V_f$ is the spacecraft floating potential, $V_{CEX}$ and $T_{CEX}$ the charge-exchange plasma potential and temperature respectively. The charge-exchange parameters are the result of the computer simulation, by setting $I_i$+$I_e$=0 we can then derive the spacecraft floating potential $V_f$ by a numerical equation solver.

### 3. Numerical Model

A three-dimensional Particle-In-Cell Code with Monte-Carlo collisions[14,15] (PIC-MCC) was developed. For Hall and Ion thrusters, ions and neutrals are treated as computer particles (one computer particle represents X real atoms) and the potential is computed from Equation (1) assuming a quasi-neutral plasma. FEEP thrusters emit an ion beam from a point or slit and therefore have very high localised plasma densities[8]. The quasi-neutral plasma assumption can be therefore not applied and the potential has to be solved using Poisson's equation on every gridpoint inside the simulation domain. An SOR solver has been implemented for this purpose.

The thruster can be either modelled alone or on top of a cubic spacecraft with a solar array attached on the side (Figure 3). The gridsize is limited by the Debye length of the embient plasma and the simulation domain is restricted by available computational resources. For Hall and Ion thruster simulations, up to 1,500,000 particles in a 2x2x2 m domain and 100x100x100 gridpoints can be calculated on a standard PC workstation. Since FEEP thrusters require additional time to solve the potential, only 300,000 particles in a 0.1x0.1x0.1 domain and up to 40x40x40 gridpoints can be simulated. Under these circumstances, the computational time to reach equilibrium is about one day.

### 4. Plasma Simulations

All electric propulsion simulations presented have been validated using available beam profile and potential measurements[7,9]. In this paper we will only concentrate on charge-exchange plasma environments, distribution of backflow currents and influence on spacecraft charging. Therefore, we first assess the plasma environment around each type of thruster, which will be the input for our spacecraft charging calculations. All density plots are evaluated through the middle of the thrusters.

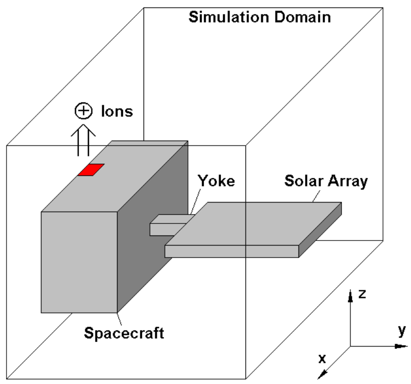


**Figure 3 Simulation Domain including Spacecraft Model**

*4.1 Hall Thruster*

The ring type emission of the SPT-100 Hall thruster causes a maximum of the ion density in the centre at a distance of about 20 cm above the thruster exit plane (Figure 4). According to our quasi-neutral plasma assumption in Equation (1), the potential distribution will follow this trend as well forming a potential hump in front of the thruster. The neutral density shows a clear asymmetry due to the propellant flowing through the neutraliser cathode (Figure 5). Combining both plots, we expect most of the charge-exchange produced close to the thruster exit plane. The potential hump at a distance of 20 cm will reflect those back to the surface which were created just below. Moreover, the positive potential from the ring type ion emission will focus them in between which we can see in the charge-exchange ion distribution shown in Figure 6.

The backflow current distribution to the surface in Figure 7 shows a clear maximum of current collected between the anode ring and a slight asymmetry around the anode due to the cathode neutral propellant flow. The charge-exchange ion density that covers the spacecraft structure is only about 1-2 orders of magnitude below the beam ion density providing. Since electrons keep this plasma quasi-neutral as well, a significant amount of electrons can interact with the spacecraft similar to a plasma contactor. As we will see later, this effect will greatly reduce spacecraft floating potentials.

*4.2 Ion Thruster*

Contrary to ring shaped anode of Hall thrusters, Ion thrusters emit a circle area shaped ion beam and do not cause a potential hump in front of the exit plane (if enough electrons are provided to form a quasi-neutral plasma of course). The beam ion densities for the UK-10 and RIT-10 Ion thrusters are shown in Figures 8 and 12 and the neutral densities in Figures 9 and 13 respectively. The charge-exchange ions are again mostly produced close to the thruster exit plane and are then strongly pushed outwards due to the positive space charge from the beam ions themselves. This creates a substantial charge-exchange environment around the thruster and rather high plasma densities close to the spacecraft surface again of 1-2 orders of magnitude below the beam plasma densities. Most charge-exchange ions are collected just outside the anode region as shown in Figures 11 and 15 respectively. We note again a slight asymmetry due to the neutral propellant flow through the neutraliser cathode.

*4.3 FEEP Thruster*

*4.3.1 Cesium FEEP*

FEEP thrusters in general have a much larger ion beam divergence than Hall or Ion thrusters due to their very small acceleration path of only < 1 mm compared to many centimetres for the others. The beam ion density for a Cs-FEEP thruster is shown in Figure 16. As discussed in the physical model, Cesium has a very high vapour pressure. Combined with the dissociation of microdroplets, the neutral density is even slightly higher then the beam ion density shown in Figure 17. However, the slit geometry causes very high localised densities. The charge-exchange ions are repelled from the positive space charge and distributed around the thruster which cases much lower densities on the grid point in the simulation. The charge-exchange ion distribution is shown in Figure 18. Since FEEP thrusters use liquid metal as propellant, the backflowing ions will stick to the surface which is different from Hall and Ion thrusters where Xenon ions only collect electrons to become neutral and are free to leave the surface again.

The backflow distribution of these ions is shown in Figure 19. The negatively biased accelerator electrode tends to collect most charge-exchange ions whereas the positive emitter slit repels them. This forms a characteristic valley distribution shape. Even though the backflow ions initially cover the surface, the high vapour pressure causes rapid thermal evaporation that causes an additional neutral environment that is not treated within this simulation.

*4.3.2 Indium FEEP*

Beam ion and neutral densities for an In-FEEP thruster are shown in Figures 20 and 21 respectively. Although ion densities between Cesium and Indium thrusters are quite comparable, the Indium neutral environment is more that 6 orders of magnitude below due to the much lower vapour pressure. This causes a very low charge-exchange ion environment being 10 orders of magnitude below beam ion densities. The positive emitter potential dominates the ion backflow distribution shown in Figure 23. However, since the accelerator electrode is grounded in this case, much fewer charge-exchange ions are attracted to the surface.

In general, FEEP thrusters cause muss less space charge potentials due to their lower emission currents compared to Hall and Ion thrusters. Electrons from thermionic neutralisers[13] have initial energies in the order of 100 to several hundred eV and hence don't see charge-exchange or beam ion space charge potentials. Therefore, FEEP thrusters will not form a quasi-neutral plasma[8] and the charge-exchange plasma will not act as a plasma contactor to lower spacecraft floating potentials.

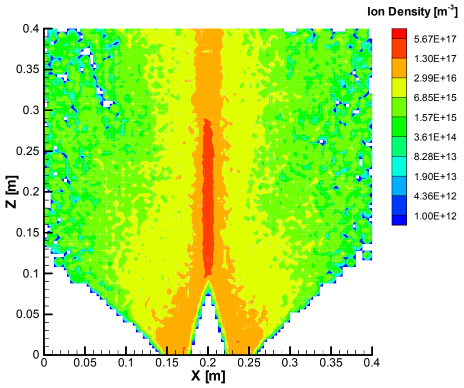


Figure 4 SPT-100 Beam Ion Density

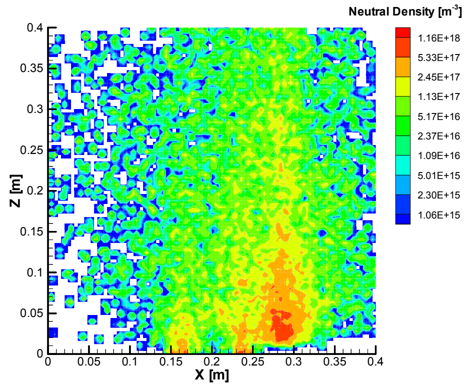


Figure 5 SPT-100 Neutral Density

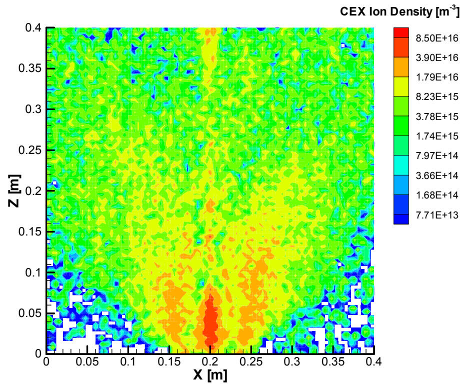


Figure 6 SPT-100 CEX Ion Density

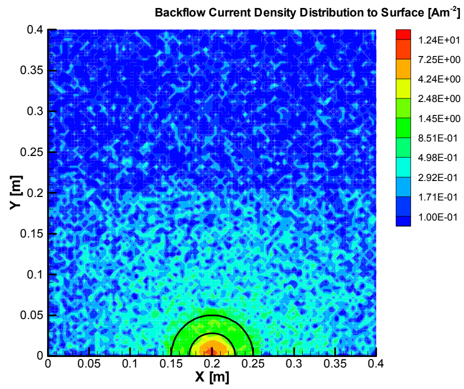


Figure 7 SPT-100 Backflow Current Distribution

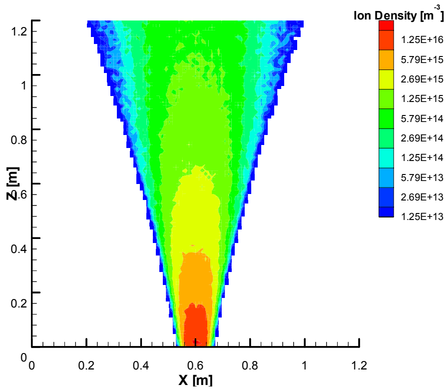


Figure 8 UK-10 Beam Ion Density

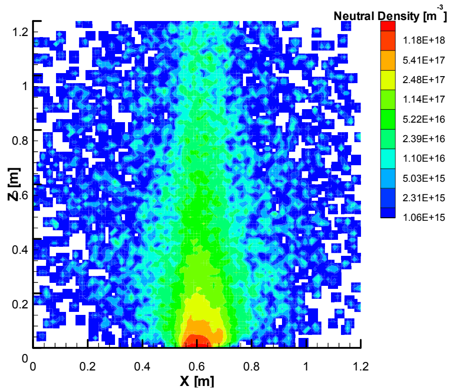


Figure 9 UK-10 Neutral Density

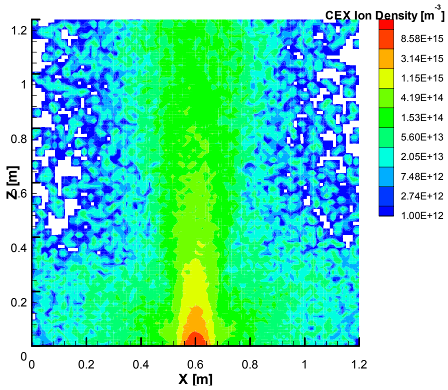


Figure 10 UK-10 CEX Ion Density

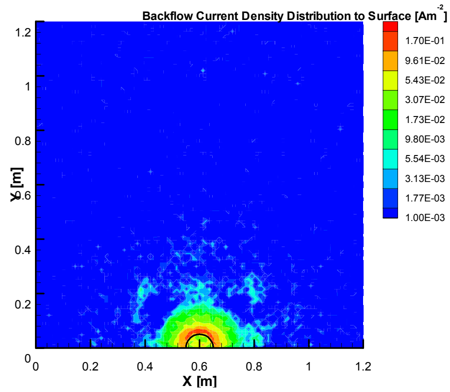


Figure 11 UK-10 Backflow Current Distribution

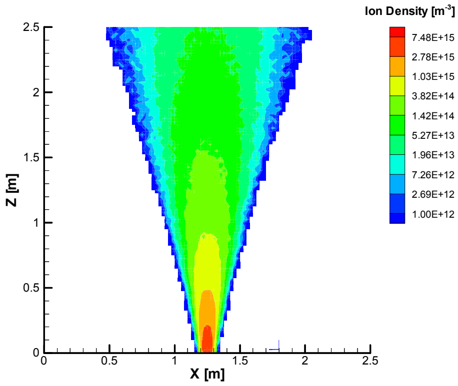


Figure 12 RIT-10 Beam Ion Density

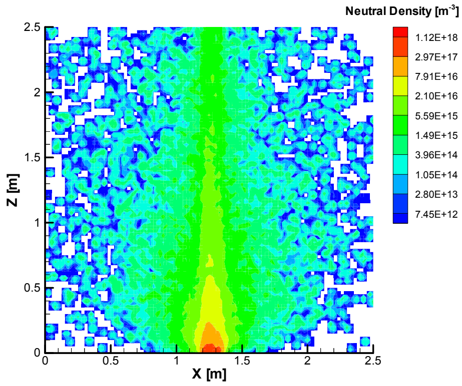


Figure 13 RIT-10 Neutral Density

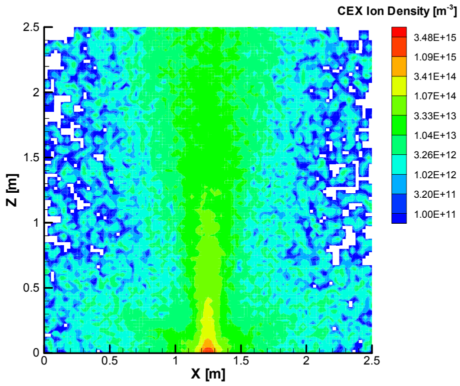


Figure 14 RIT-10 CEX Ion Density

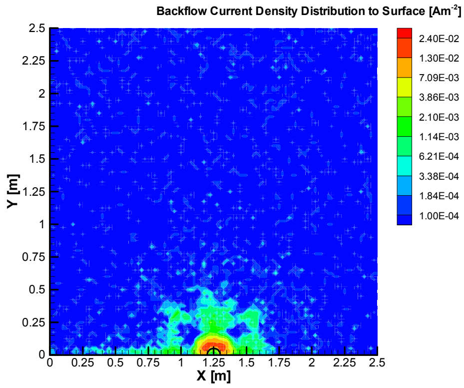


Figure 15 RIT-10 Backflow Current Distribution

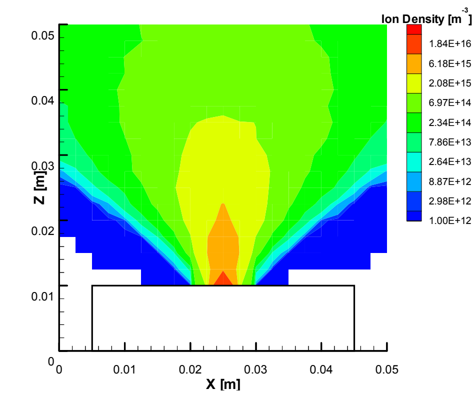


Figure 16 Cs-FEEP Beam Ion Density

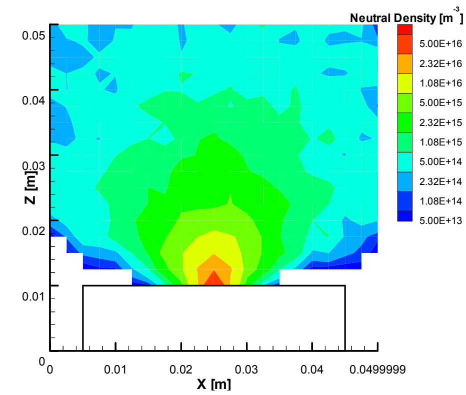


Figure 17 Cs-FEEP Neutral Density

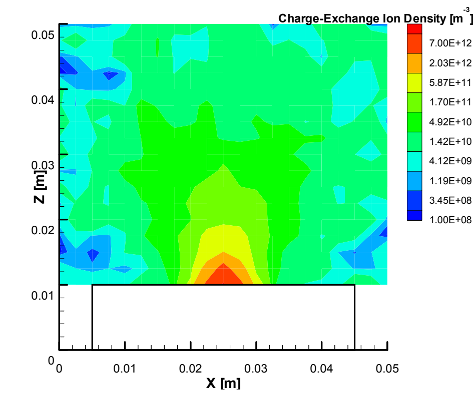


Figure 18 Cs-FEEP CEX Ion Density

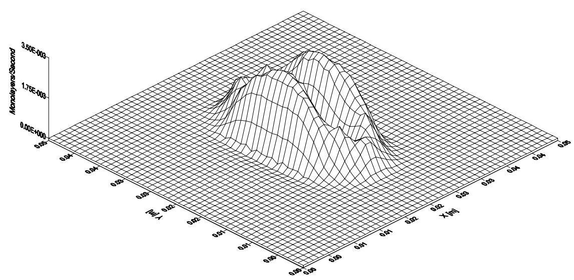

Figure 19 Cs-FEEP Backflow Monolayer Distribution

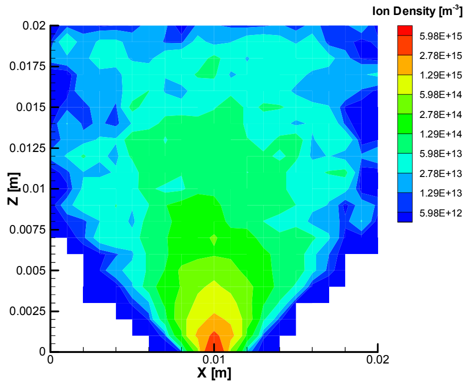


**Figure 20 In-FEEP Beam Ion Density**

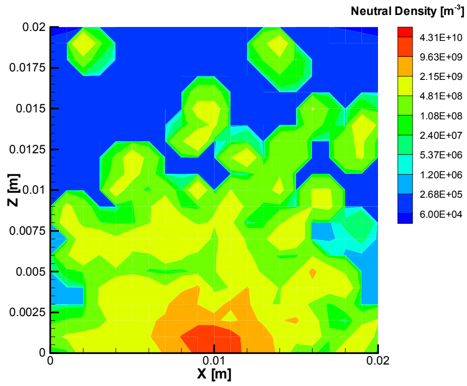


**Figure 21 In-FEEP Neutral Density**

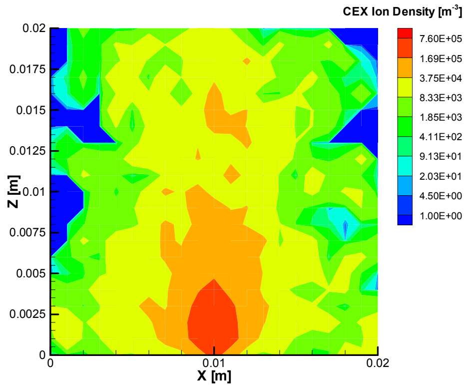


**Figure 22 In-FEEP CEX Ion Density**

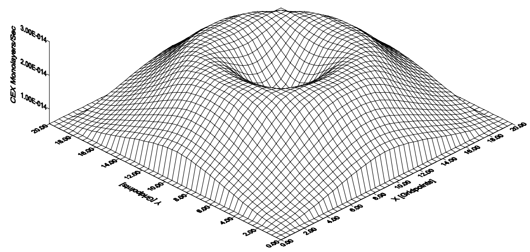

**Figure 23 In-FEEP Backflow Monolayer Distribution**

## 5. Backflow and Spacecraft Charging Calculations

The backflow current distribution was integrated along the spacecraft surface summarised in Table 3 for the various electric propulsion thrusters. The SPT-100 Hall thruster has a backflow to emission current ratio of about 0.8%. The Ion thrusters have a bit lower ratios of around 0.2%. This is consistent with backflow predictions for NASA's NSTAR Ion thruster[16]. FEEP thrusters have much less backflow ratios of $2x10^{-2}$% for the Cesium and only $7x10^{-8}$% for the Indium FEEP respectively. This is due to the lower ion and neutral densities produced by the much lower emission currents compared to Hall and Ion thrusters. This leads at least to a square root behaviour of charge-exchange production to emission current[5,9]. Moreover, in the Indium-FEEP case, the atomic neutral environment is simply too low to cause significant charge-exchange collisions. Equation (3) is solved to compute the spacecraft floating potential $V_f$ assuming a cubic spacecraft of 1x1x1 m moving at orbital velocity of 8 km/s. Also the ion emission and neutraliser currents are assumed to the equal which is generally not always the case. Three different ambient conditions are evaluated: vacuum, LEO and GEO orbital conditions (parameters summarised in Table 4). All spacecraft floating potentials are shown in Table 5. In all cases an electron temperature of 1 eV was assumed for the charge-exchange plasma which is lower than the fixed electron temperature in the beam (3-5 eV) due to the lower CEX plasma densities.

| | Emission Current $I_E$ | Backflow Current $I_B$ | $I_B/I_E$ Ratio |
|---|---|---|---|
| SPT-100 | 4100 mA | 32 mA | 0.78 % |
| UK-10 | 440 mA | 1.02 mA | 0.23 % |
| RIT-10 | 210 mA | 0.35 mA | 0.16 % |
| Cs-FEEP | 5 mA | $9.3x10^{-4}$ mA | $1.9x10^{-2}$ % |
| In-FEEP | 0.25 mA | $1.8x10^{-10}$ mA | $7.2x10^{-8}$ % |

**Table 3 Backflow Currents at typical Operating Conditions**

| | Plasma Density | Electron Temperature | Ambient Ion Mass |
|---|---|---|---|
| LEO | $10^{12}$ m$^{-3}$ | 0.1 eV | $2.66x10^{-26}$ kg |
| GEO | $10^{6}$ m$^{-3}$ | 1000 eV | $1.66x10^{-27}$ kg |

**Table 4 Ambient Plasma Conditions**

|  | Spacecraft Floating Potential [V] |  |  |
|---|---|---|---|
|  | Vacuum | LEO | GEO |
| No Thruster | 0 | -0.35 | -3744.6 |
| SPT-100 | -16.3 | -16.2 | -16.3 |
| UK-10 | -6.5 | -5.6 | -6.5 |
| RIT-10 | -8.9 | -7.3 | -9.1 |
| Cs-FEEP | - | -0.35 | -2645 |
| In-FEEP | - | -0.35 | -3744.6 |

**Table 5 Spacecraft Floating Potentials at typical EP Operating Conditions**

With no thruster firing, the floating potentials in LEO are slightly different from vacuum, in our case $V_f$ = -0.35 V. Due to the much higher electron temperatures of keV in GEO orbit (solar wind, etc.), the floating potentials can obtain several thousand Volt negative.Operating an electric propulsion thruster, the charge-exchange plasma will act as a plasma bridge between the spacecraft surface, the ion beam and the neutraliser electrons. In that case the floating potential is reduced from –3744 Volts to –16 or even down to –6 Volts for the Hall and Ion thrusters respectively. The difference between GEO and vacuum thruster operation is neglectible due to the already very low plasma densities in GEO of $10^{-6}$ $m^{-3}$.

In the case of LEO orbit, the CEX plasma contact causes a slightly more negative floating potential from the initial –0.35 V due to the lower ambient electron temperature of only 0.1 eV. These floating potential values of around –10 Volt have actually been measured in space experiments using Ion thrusters on the experimental ATS-6 spacecraft[17].

The very low backflow currents from FEEP thrusters do not change the LEO floating potentials. Contrary to Hall and Ion thrusters, a FEEP thruster does not need a neutraliser to reduce space charge necessary for operation. Since the FEEP plasma is not quasi-neutral and the neutraliser electrons usually do not couple to the CEX ions[8], FEEP thrusters do not act as a plasma contactor. This makes it impossible to evaluate the spacecraft floating potential in vacuum since the positive backflow current is not balanced by an electron current flowing to the surface. In reality, electrons will be attracted by changed spacecraft floating potentials to counterbalance this effect. However, due to the limited simulation domain, this effect could not be modelled. Therefore, also the GEO floating potential values for FEEP thruster operation are only partially correct although the ambient plasma can supply electrons in this case.

Since the spacecraft floating potential remains unchanged in LEO orbits with and without thruster operation, a neutraliser for FEEP thrusters is not always necessary to maintain the spacecraft floating potential. The ambient electron current (order or tens of mA) is usually at least one order of magnitude higher that the one required for a FEEP thruster (in our example 0.25 for In-FEEP and 5 mA for the Cs-FEEP respectively). Depending on the spacecraft orbit, spacecraft size and amount of FEEP thrusters at certain thrust levels, the model can be used to predict the change of the spacecraft floating potential. In case of marginal change, the neutraliser can be abandoned saving power, mass and volume.

## 6. Summary

A 3D numerical Particle-In-Cell simulation was developed to model Hall, Ion and FEEP thrusters operation on board a spacecraft. Backflow currents were shown to be below 1% of the emitted current for all thrusters. Charge-exchange plasmas produced by Hall and Ion thrusters were shown to act similar to a plasma contactor and are able to significantly reduce the spacecraft floating potential from several thousand Volts negative in GEO to around –10 Volt. FEEP thrusters do not couple electrons to their charge-exchange ions and hence are not able to reduce spacecraft floating potentials significantly. Depending on orbits and total thrust, the model suggests that a neutraliser is not always necessary for spacecraft equipped with FEEP thrusters.

## References

[1]Saccoccia, G., González del Amo, J., and Estublier, D., "Electric Propulsion: A Key Technology for Space Missions in the New Millenium", ESA Bulletin, **101**, 2000

[2]Racca, G.D., Foing, B.H., and Rathsman, "An Overview on the Status of the SMART-1 Mission", *International Astronautical Congress*, IAA-99-IAA.11.2.09, 1999

[3]Bassner, H., Berg, H.P., Fetzer, K., and Müller, G., "Ion Propulsion Package IPP for N/S-Stationkeeping of the ARTEMIS Satellite", *International Electric Propulsion Conference*, IEPC-91-055, 1991

[4]Bonnet, J., Marque, J.P., and Ory, M., "Development of a Thrust Balance in the Micronewton Range", *3rd International Conference on Spacecraft Propulsion*, 2000

[5]Tajmar, M., Rüdenauer, F., and Fehringer, M., "Backflow Contamination of Indium Liquid-Metal Ion Emitters (LMIE): Numerical Simulations", *International Electric Propulsion Conference*, IEPC-99-070, 1999

[6]Tajmar, M., Gonzales, J., and Hilgers, A., "Modelling of Spacecraft-Environment Interactions on SMART-1", *AIAA Joint Propulsion Conference*, AIAA 2000-3526, 2000

[7]Tajmar, M., Gonzalez, J., Estublier, D., and Saccoccia, G., "Modelling and Experimental Verification of Hall and Ion Thrusters at ESTEC", 3rd International Conference on Spacecraft Propulsion, 2000

[8]Tajmar, M., and Wang, J., "3D Numerical Simulation of Field-Emission-Electric-Propulsion Neutralization", *Journal of Propulsion and Power*, Vol. 16, No. 3, 2000, pp. 536-544

[9]Tajmar, M., and Wang, J., "3D Numerical Simulation of Field-Emission-Electric-Propulsion Backflow Contamination", *Journal of Spacecraft and Rockets*, **38**(1), 2001, pp. 69-78

[10]Marcuccio, S., Genovese, A., and Andrenucci, M., "Experimental Performance of Field Emission Microthrusters," *Journal of Propulsion and Power*, **14**(5), 1998, pp. 774-781

[11]Steiger, W., Genovese, A., and Tajmar, M., "Micronewton Indium FEEP Thrusters", *3rd International Conference on Spacecraft Propulsion*, 2000

[12]Mitterauer, J., "Field Emission Electric Propulsion Spectroscopic Investigations on Slit Emitters," Vienna University of Technology, Final Report on ESTEC-Contract 5051/82/NL/PB (SC), Dec. 1985

[13]Fehringer, M., Rüdenauer, F., and Steiger, W., "Micronewton Indium Ion Thrusters", *International Electric Propulsion Conference*, IEPC-99-6, 1999

[14]Birdsall, C.K., and Langdon, A.B., "Plasma Physics via Computer Simulation", Institute of Physics Publishing, 1991

[15]Birdsall, C.K., "Particle-in-Cell Charged-Particle Simulations, Plus Monte Carlo Collisions With Neutral Atoms, PIC-MCC", *IEEE Transactions on Plasma Science*, **19**, No. 2, April 1991

[16]Samanta Roy, R.I., Hastings, D.E., and Gatsonis, N.A., "Numerical Study of Spacecraft Contamination and Interactions by Ion-Thruster Effluents", *Journal of Spacecraft and Rockets*, **33**(4), 1996, pp. 535-542

[17]Olsen, R.C., "Modification of Spacecraft Potentials by Plasma Emission", *Journal of Spacecraft*, **18**(5), 1981, pp. 462-469